

Realistic Inflow Conditions for Numerical Green Water Simulations

Geert Meskers *

R.H.M.Huijsmans

r.h.m.huijsmans@marin.nl †

January 14, 2003

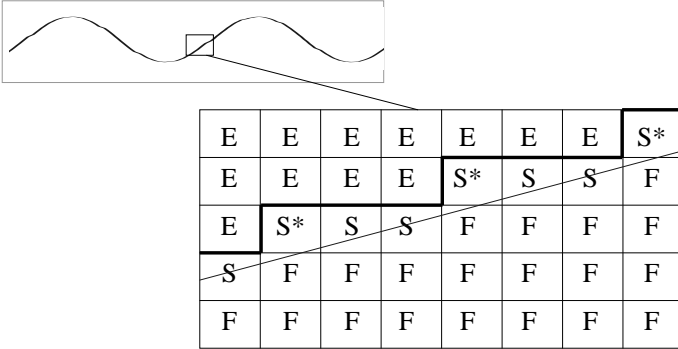


Figure 1: Close-up of the cell labeling at the wave surface.

Abstract

To model realistic inflow conditions for green water simulations, a free floating ship in a non-linear realistic wave field should be modeled. First the extension of the numerical tool with a realistic wave field is investigated. The simulation of non-linear realistic waves in the VOF code is investigated with special attention to the artificial boundaries used to limit the computational domain.

Boundary conditions

For the discretisation of Laplace all velocities on the cell faces has to be known. Therefore, the *FB*-velocities need to be prescribed. For the discretisation of momentum equation, not only the *FB*-velocities, but also the *SB*-velocities, *BB*-velocities, the *SE*-velocities and the *EE*-velocities adjacent to a *SS*-velocity need to be prescribed. Further, the pressures on either side of the velocity around which the momentum equation is discretised, is needed. This means that to discretise the momentum equation around *FS*- and *SS*-velocities the pressure in the *S*-cells needs to be prescribed.

The *FB*-, *SB*- and the *BB*-velocities are prescribe using the no-slip or free-slip conditions on solid boundaries. When the boundary acts as an artificial boundary it should also prescribe the *FB*-, *SB*- and the *BB*-velocities, this is discussed in the next section.

The *SE*-velocities and the *EE*-velocities adjacent to a *SS*-velocities and the pressure in *S*-cells are prescribed us-

ing the free surface conditions. The *EE*-velocities are prescribed using the surface stresses. In 2D this equation is simplified to:

$$\mu \left(\frac{\partial u_x}{\partial z} + \frac{\partial u_x}{\partial z} \right) = 0 \quad (1)$$

assuming a either horizontal or vertical surface. The *SE*-velocities are in general prescribe by applying conservation of mass in the *S*-cell. When two *SE*-velocities occur around one *S*-cell, conservation of mass is required in each direction separately. During the accuracy tests for wave simulation this was found to be introducing inaccuracies. A little sloping surface like the surface of a ocean wave, cause a staircase like *S*-cell pattern, see Fig. 1. Besides vertical *SE*-velocities, this also cause some horizontal *SE*-velocities. Here there are two *SE*-velocities in around one *S*-cell (marked with * in Fig. 1), thus in this case where no cut-cells are present, both *SE*-velocities are set equal to the opposite velocity. This means both $\frac{\partial u_x}{\partial x} = 0$ and $\frac{\partial u_x}{\partial x} = 0$. However in the steepest part of the wave where this is likely to happen, $\frac{\partial u_x}{\partial x}$ is not equal to zero but at it's maximum. This error is circumvented by prescribing the horizontal *SE*-velocities in wave simulations the same way the *EE*-velocities are prescribed. This implies the assumption of a more or less horizontal surface.

Simulating a Wave Field

To extend the current model for numerical green water simulations with a wave field, first the capabilities of Comflo to simulate a non-linear realistic wave field accurately without the presence of an object is investigated. The propagation of the waves inside the computational domain is important, but also the influence of the boundaries are investigated.

Accuracy of the Simulations

To get an idea of the accuracy and the required grid resolution and time step for wave simulations a series of computations is performed. Regular waves are simulated by prescribing the velocities at the boundaries using the non-linear potential theory of Rienecker-Fenton, [1] see the next section. A 2D domain of 2 wavelengths is used, the wave elevation is determined in middle of the domain and compared with the Rienecker-Fenton results over two wave periods. In other computations it was found that a grid aspect ratio, $\Delta z / \Delta x$, (much) different from 1.0, can cause wiggles for

*Technical University Delft

†Maritime Research Institute Netherlands

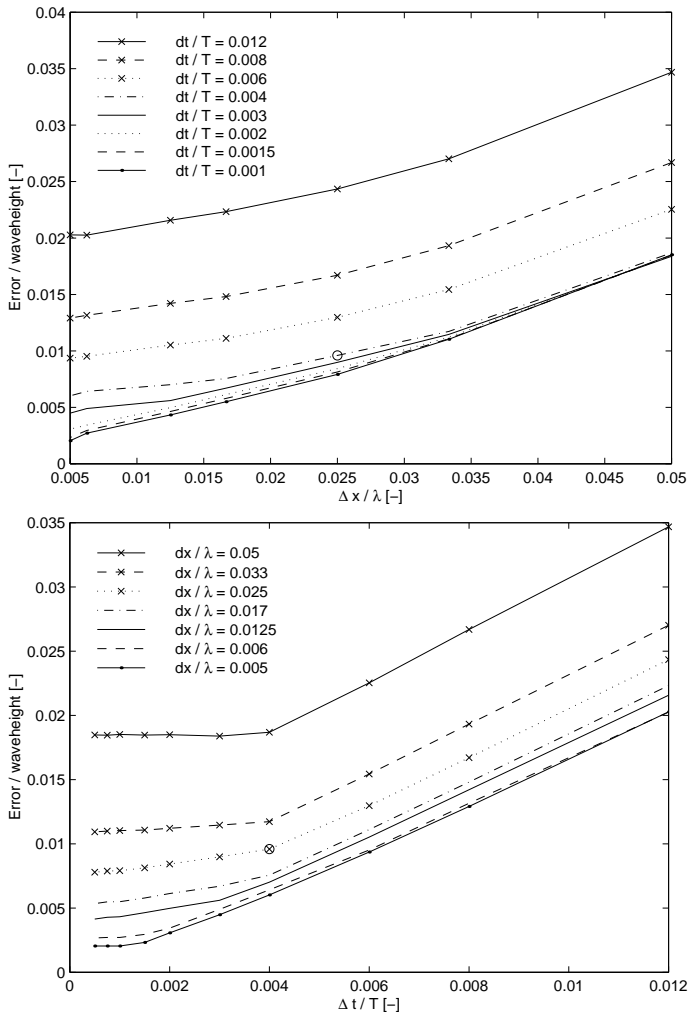


Figure 2: Influence of grid resolution and timestep on the accuracy of wave simulations, wave steepness $H/\lambda = 0.02$

step waves. Therefore, the grid aspect ratio is kept equal to 1.0.

In Fig. 2 the maximum error found by comparing the time traces of the numerical simulation and the Rienecker-Fenton theory is plotted for different grid resolutions and time steps. These results are obtained for a wave with steepness $H/\lambda = 0.02$. Clearly the error is linearly depending on the timestep up to a point where the spatial discretisation error is more important, then the time step refinement has almost no influence anymore. For steeper waves the general behaviour of the error is the same. However, the graphs are shifted towards a finer grid. For the same accuracy of the simulation of a steeper wave approximately the same amount of time steps can be used, but more grid cells are necessary. This is probably due to the fact that nonlinear wave components with the same period but a halved or even less wave length are larger. In table 1 the optimum choice of parameters for an error of 1% of the waveheight is given for different wave steepness. It also gives the computation time on a 500 MHz PC per wave length and per wave period, which drastically increases for steeper waves.

H/λ	$\Delta t/T$	$\Delta x/\lambda$	comp. time [min]
0.02	0.004	0.025	0.4
0.04	0.004	0.0125	1.4
0.06	0.004	0.0083	4.3
0.08	0.003	0.0063	11.3
0.10	0.0015	0.005	26.4

Table 1: 'Optimum' choice of parameters for an allowed error of 1% of the wave height and computational time per wave length and wave period.

Artificial Boundaries

To limit the computational domain, artificial boundaries are introduced. When the artificial boundary acts as an inflow boundary the velocities of the incoming wave field should be prescribed to the computational domain. When the artificial boundary acts as an outflow boundary, it should absorb the outgoing waves as if no boundary is present. Two absorbing methods are presented here, the Sommerfeld condition and an absorbing damping zone. Often the inflow also acts as an outflow boundary for reflected or diffracted waves. In this case the in- and outflow conditions should be combined. The possibilities to remove the artificial boundaries by coupling the computational domain with the outer domain, while the solution in the outer domain is computed using a potential code is also investigated.

Inflow Condition

At the inflow boundary the incoming wave should be prescribed by prescribing the velocity profile of the wave at the boundary. Hereto a good description of the incoming wave is necessary. For low amplitude waves, both regular and irregular, the Airy linear potential wave theory provides an accurate description. Using a linear theory implies that the velocity profile is only computed up to the calm water level. In the nonlinear VOF code the velocities need to be prescribed up to the actual surface level. To overcome this problem a profile stretching method is used. It was found that simply extrapolate the linear profile up to the actual surface level worked well. An alternative method is Wheeler stretching, [3], which stretches or compresses the velocity profile from the calm water level to the actual surface level.

When the wave steepness increases nonlinear effects cause deviations from the linear theory. At a wave steepness of $H/\lambda = 0.02$ deviations in the surface elevation are already about 3% of the wave amplitude. For accurate wave simulations a nonlinear description of the incoming wave should be used. Rienecker and Fenton provided a relatively simple method to get a nonlinear potential description of a regular wave in any water depth by means of a Fourier series of the stream function. This is a very suitable method for regular nonlinear waves. For irregular nonlinear waves no analytical description can be given. In this case the velocity profile at the boundary during the simulated time is computed using a nonlinear potential code based on the Finite Element Method (FEM). First the full domain is computed

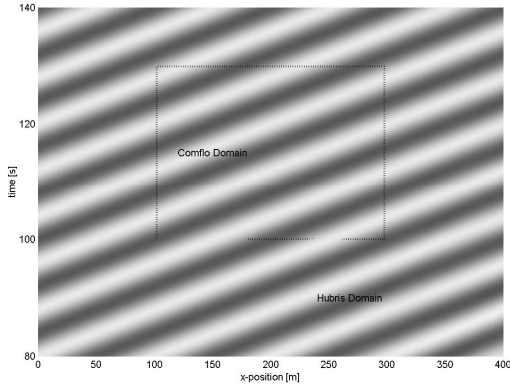


Figure 3: Position time plot of the results of the nonlinear FEM code Hubris and the VOF-code Comflo initiated by Hubris on $t = 100s$ and driven by Hubris on $x = 100m$.

by the FEM code, the results on $t = 100s$ and on $x = 100m$ are prescribed to the VOF code. Comparison at $x = 250m$ and at $t = 140s$ shows no large discrepancies exist between the solution of the FEM-code and of the VOF-code driven by the FEM-code. The same check is performed for the FEM-code driven by the VOF-code on $x = 100m$ (in this case no initial condition) by prescribing the time derivative of the potential on the boundary. The results of this check encourages future investigation of an interactive coupling so the potential FEM-code can also be used as an outflow boundary.

Sommerfeld Condition

A well known outflow condition is the Sommerfeld condition. The Sommerfeld condition is based on the wave equation and can be applied to properties that satisfy the wave equation. In this case the Sommerfeld condition is applied to the velocity components of the fluid:

$$\frac{\partial u}{\partial t} = -c \frac{\partial u}{\partial x} \quad (2)$$

$$\frac{\partial w}{\partial t} = -c \frac{\partial w}{\partial x} \quad (3)$$

in three dimensions an extra equation for the velocity component in y -direction, v , is added. A wave traveling with wave speed c is fully absorbed by this condition. Therefore, the Sommerfeld condition is very useful for regular wave simulation, where it can be tuned to absorb the wave exactly. Waves with a slightly different wave speed are partially reflected. This reflection is analytically found to be:

$$r = \left| \frac{c_s - \omega/k}{c_s + \omega/k} \right| \quad (4)$$

With the reflection coefficient r defined as the fraction between the amplitude of the reflection and the original amplitude, $r = \frac{\zeta_{refl}}{\zeta_{orig}}$. In Fig. 4 and Fig. ?? the reflection coefficients found numerically are compared with the analytical values of Eq. 4 for deep water and shallow water respectively.

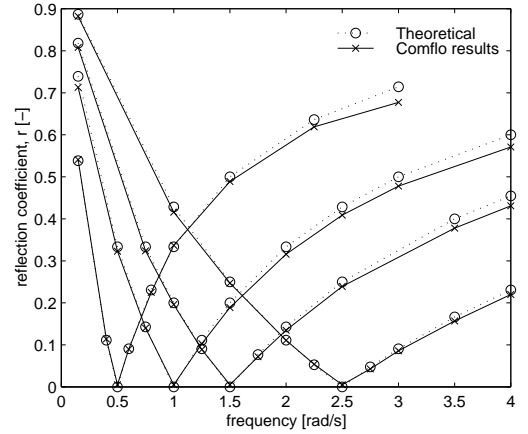


Figure 4: Reflections found using the Sommerfeld condition tuned for different wave frequencies on deep water compared with theoretical results.

It shows that the Sommerfeld condition works as expected. It perfectly absorbs one frequency and is thus very suitable for regular wave simulations. For irregular waves the Sommerfeld condition can be used to absorb the peak period and a large part of the other periods, or to absorb the long shallow water wave. However, the Sommerfeld condition alone is not enough to absorb a full wave spectrum.

Solitary wave splitting

To investigate the ability of the VOF based Navier Stokes solver to simulate nonlinear phenomenon, the splitting of a solitary wave (or soliton) propagating over an uneven bottom is simulated.

Because the propagation and splitting of a soliton is a subtle balance between dispersion and nonlinearity, Westhuis [2] used the propagation of a soliton over uneven bottoms to test the ability of his nonlinear finite element code to simulate both these aspects.

The soliton is propagating reasonable steady, although the height is slowly increasing as it propagates. This was not found in the experiments of Westhuis, where a steady soliton with a height of 0.102 m was obtained over a long domain. This discrepancy could be caused by the empirical initial condition. The propagation speed of 2.429m/s is in good agreement with the speed found by Westhuis, 2.427m/s, and the theoretical values of Boussinesq and Korteweg-de Vries respectively 2.426m/s and 2.436m/s.

For the simulation of a soliton splitting into three solitons, the bottom rises from $-0.5m$ to $-0.25m$ between $x = 20m$ and $x = 30m$. A square grid of $dx = 0.025$ is used, which showed accurate for the even bottom case. Due to the sloping bottom the velocity increases, to limit the CFL-number the time step is therefore halved to $dt = 0.005$. Snapshots of the splitting at a number of time levels are shown in Fig. 6. The steepening of the soliton at the bottom slope is clearly shown, although the final height of 16.4m found by Westhuis for the largest soliton is not reached. Further, the

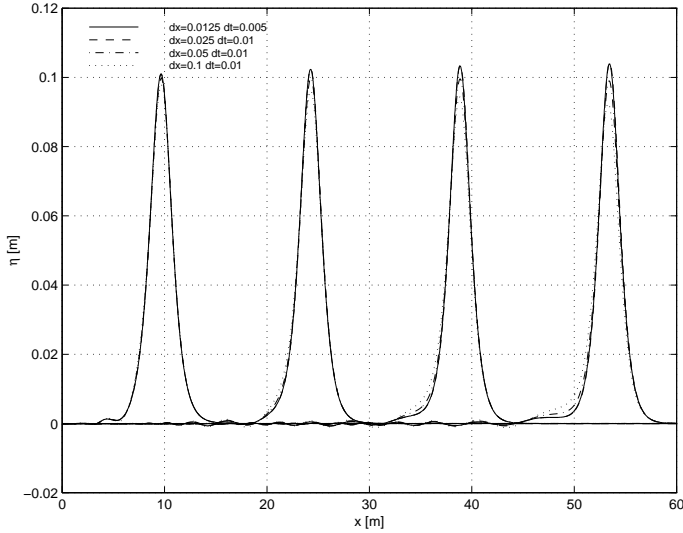


Figure 5: Snapshots of a soliton propagating over an even bottom on $t = 4s, t = 10s, t = 16s$ and $t = 22s$, for different grid sizes.

height of the largest soliton drops rapidly while propagating. This indicates that an even finer grid is necessary in the shallow water region, which could also be the cause that the largest soliton doesn't reach his final height. Also the splitting process in the shallow water region is captured by the simulations, a second soliton is detached from the first and also a third soliton is clearly developing. The second soliton is also a bit lower than the one found by Westhuis, $0.049m$ against $0.0538m$. However, the height of this soliton is still increasing, so it might not be fully developed yet.

It can be concluded that the present method is capable of simulating even subtle nonlinear phenomenon like the propagation and splitting of a soliton. However, to accurately capture the steepening of the main soliton a finer grid should be applied. And to fully capture the splitting process a longer domain is necessary. For these measures the computational resources were not available. The development of a multi block algorithm for problems like these, when a finer grid resolution is required in part of the domain, could increase the effectiveness of the method and is therefore highly recommended.

References

- [1] M.M. Rienecker and J.D. Fenton. A fourier approximation method for steady water waves. *Journal of Fluid Mechanics*, 104:119, 1981.
- [2] J. Westhuis. *The Numerical Simulation of Nonlinear Waves in a Hydrodynamic Model Test Basin*. PhD thesis, University of Twente, 2001.
- [3] J.D. Wheeler. Method for calculating forces produced by irregular waves. *Journal of Petroleum Technology*, 1970.

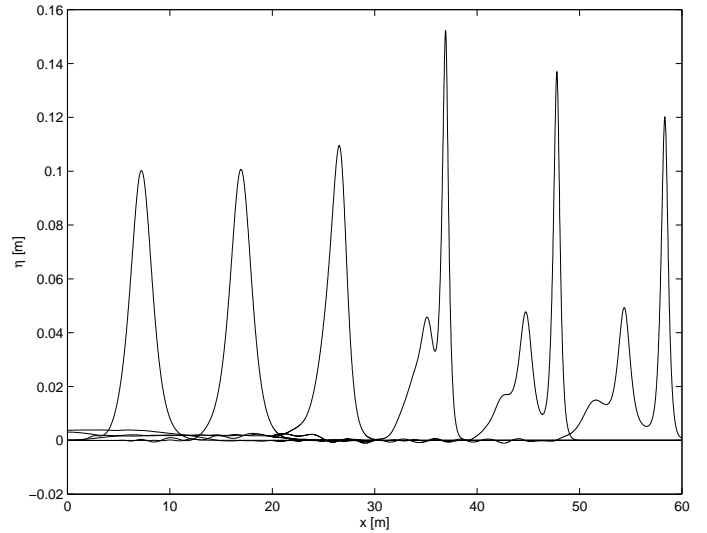


Figure 6: Snapshots of a soliton propagating over uneven bottom on $t = 3s, t = 7s, t = 11s, t = 16s, t = 21.5s$ and $t = 27s$.